# Structural models of genome-wide covariance identify multiple common dimensions in autism

Lucía de Hoyos[1], Maria T Barendse[1,2], Fenja Schlag[1], Marjolein MJ van Donkelaar[1], Ellen Verhoef[1], Chin Yang Shapland[3,4], Alexander Klassmann[5], Jan Buitelaar[6-8], Brad Verhulst[9], Simon E Fisher[1,6], Dheeraj Rai[4,10,11], Beate St Pourcain[1,3,6 *]

Affiliations

[1] Language and Genetics Department, Max Planck Institute for Psycholinguistics, Nijmegen, The Netherlands

[2] Department of Social Dentistry and Behavioural Sciences, Academic Centre for Dentistry Amsterdam (ACTA), Amsterdam, The Netherlands

[3] MRC Integrative Epidemiology Unit, University of Bristol, Bristol, United Kingdom

[4] Population Health Sciences, University of Bristol, Bristol, United Kingdom

[5] Institute for Genetics, University of Cologne, Cologne, Germany

[6] Donders Institute for Brain, Cognition and Behaviour, Radboud University, Nijmegen, The Netherlands

[7] Karakter Child and Adolescent Psychiatry University Centre, Nijmegen, The Netherlands

[8] Department of Cognitive Neuroscience, Radboud University Medical Center, Nijmegen, The Netherlands

[9] Texas A&M University, College Station, TX, United States

[10] Avon and Wiltshire Partnership NHS Mental Health Trust, Bristol, United Kingdom

[11] NIHR Biomedical Research Centre, University of Bristol, Bristol, United Kingdom

* corresponding author

Email: Beate.StPourcain@mpi.nl

## Abstract

Common genetic variation has been associated with multiple symptoms in Autism Spectrum Disorder (ASD). However, our knowledge of shared genetic factor structures contributing to this highly heterogeneous neurodevelopmental condition is limited. Here, we developed a structural equation modelling framework to directly model genome-wide covariance across core and non-core ASD phenotypes, studying autistic individuals of European descent using a case-only design. We identified three independent genetic factors most strongly linked to language/cognition, behaviour and motor development, respectively, when studying a population-representative sample (N=5,331). These analyses revealed novel associations. For example, developmental delay in acquiring personal-social skills was inversely related to language, while developmental motor delay was linked to self-injurious behaviour. We largely confirmed the three-factorial structure in independent ASD-simplex families (N=1,946), but uncovered simplex-specific genetic overlap between behaviour and language phenotypes. Thus, the common genetic architecture in ASD is multi-dimensional and contributes, in combination with ascertainment-specific patterns, to phenotypic heterogeneity.

# INTRODUCTION

Autism spectrum disorder (ASD) is a complex neurodevelopmental condition with considerable phenotypic and genetic heterogeneity (1,2). Core phenotypes in ASD implicate difficulties in social interaction and communication, as well as restricted, repetitive behavioural patterns and sensory abnormalities (3). However, the phenotypic presentation is broad and variable. More than 70% of individuals with ASD are diagnosed with co-occurring conditions (henceforth referred to as ASD phenotypic spectrum) (4), and individuals differ in phenotypic presentation, especially cognitive functioning (2,4). At the genetic level, additive genetic effects of rare and common genetic factors contribute to ASD liability in a sex-specific manner (1,5–10). Common variation explains most genetic variance in ASD, accounting for 12 to 65% of liability (1,5,11). However, even common genetic variation is highly heterogenous in ASD (5,6,8), and differences in underlying shared genetic factors are only partially understood.

Depending on an individual's genetic architecture, common variants act through partially distinct aetiological mechanisms (6). For example, autistic individuals with intellectual disability (ID), compared to those without, carry a higher rate of contributing *de novo* variants (6) and show qualitative differences in their common genetic architecture (5). In addition, polygenic scores (PGS) for different disorders, aggregating common risk alleles, show distinct association profiles with phenotypic factor structures in groups comprising only autistic individuals (8,12). Thus, also common variation may present genetic factor structures linking phenotypic domains, although the number of factors and their nature is unknown. Furthermore, the genetic architecture of ASD is distinctly different in multiplex families with multiple affected family members, compared to simplex families with only one affected child (13). ASD liability in simplex families is considerably more often related to *de novo* mutations (11,14). Therefore, also common genetic factor structures may differ between exclusively simplex and population-representative ASD architectures, where latter contain both simplex and multiplex families.

This study applies genetic-relationship-matrix (GRM) structural equation modelling (GRM-SEM) techniques to identify and characterise shared genetic factor structures in autistic individuals from large ASD cohorts adopting a case-only design (**Figure 1**). GRM-SEM estimates multivariate common genetic architectures (15), as captured by GRMs derived from direct genotyping data (15,16), by directly fitting structural models to genetic and residual variation using a maximum likelihood (ML) approach (15). Consequently, models can be compared with and optimised against a saturated model, i.e. a model with a perfect fit (15). Here, we introduce a

data-driven version of GRM-SEM (**Figure 1B**) that minimises the computational burden of identifying the best-fitting multi-dimensional model. We predict the number of genetic factors and their structure from genetic trait covariance, as estimated with a saturated GRM-SEM model, using principal component analysis (PCA) and exploratory factor analysis (EFA) techniques. Given the estimated nature of these genetic data, conducted analyses are approximations only, henceforth referred to as genetic PCA and genetic EFA, respectively. We use genetic PCA and EFA information to identify a multi-dimensional GRM-SEM model by providing starting values and parameter constraints.

We implement this data-driven modelling strategy into a multi-stage research design to examine the genetic architecture of ASD across a broad range of related phenotypes and comorbidities, studying the most well-characterised ASD cohorts to date. As part of discovery analyses, we investigate ASD core and non-core phenotypes for 5,331 European descent individuals with ASD from the Simons Foundation Powering Autism Research for Knowledge (SPARK) sample (17) (**Supplementary Table 1, Supplementary Figure 1, Supplementary Methods 1**). Recruited across the United States (US), SPARK is a population-representative ASD sample including individuals from simplex or multiplex families (17). We follow up our results on 1,946 autistic individuals from simplex-only families of the Simons Simplex Collection (SSC) sample (18) (**Supplementary Table 2, Supplementary Figure 2, Supplementary Methods 2**). Here, we report and contrast comprehensive multivariate genetic models estimated in SPARK and the SSC, empowering new insights into the heterogeneous phenotypic spectrum of ASD across samples representing different ascertainment schemes.

# RESULTS

## Multi-dimensional genetic analyses in population-representative ASD

A challenge in identifying the genetic architecture of ASD core and non-core phenotypes is the selection of measures for model building. We, therefore, conducted discovery analyses in the population-representative SPARK sample across multiple stages (**Figure 1**). During stage I, we screened for phenotypes that are likely to have some genetic contributions ($h^2_{SNP}$, $p \leq 0.1$, **Figure 2A**), using Genomic Restricted Maximum Likelihood (GREML) embedded in GCTA software (19,20), to ensure the convergence of GRM-SEM models. Note that $h^2_{SNP}$ estimates in this study reflect phenotypic heterogeneity among autistic individuals that can be accounted for

by common genetic variation. We retained 17 phenotypes from an initial set of 47 phenotypes, disorders and developmental milestones (**Figure 2A**). Captured domains included language/cognition, general behaviour, developmental, motor and repetitive behavioural features. Social and affective phenotypes were not taken forward to the next stage of analysis due to a lack of evidence for $h^2_{SNP}$ (**Supplementary Figure 3**). Next, we screened for phenotype combinations that are possibly sharing common genetic variation ($r_g$ $p \leq 0.1$, **Figure 2B**) to enable the identification of overarching genetic factors.

Within stage II, we selected phenotypic subsets that jointly captured estimated genetic correlations from stage I, based on an enumeration of phenotype combinations, with the aim to successively construct a comprehensive GRM-SEM model (**Figure 2B**, **Supplementary Figure 4**, **Supplementary Table 3**, **Supplementary Note 1**). Building a model from smaller phenotypic subsets ensures the robustness of identified structures and reduces the computational burden. The most extensively genetically linked phenotypic subsets were related to language disorder (including developmental language disorder/delay, $S_{DLD}$), language level ($S_{LL}$) and age of crawling ($S_{CRL}$), respectively (**Figure 2B**). To control for measurement collinearity that can affect model convergence, we searched, in addition, for genetically correlated scales within a questionnaire using uni-dimensional GRM-SEM (**Supplementary Note 1**, **Supplementary Figure 5**). Where item scales of the same instrument were genetically similar (GRM-SEM $r_g$=1), we retained a single representative measure (or proxy) only (**Figure 2B, Supplementary Note 1**, **Supplementary Figure 5**).

As part of stage III, we aimed to identify the best-fitting multi-dimensional GRM-SEM models for the selected phenotypic subsets and, eventually, a combined set of measures, $S_{ALL}$ (**Supplementary Note 2**). For this, we fitted a series of GRM-SEM saturated (Cholesky) models, genetic PCA eigenvalue decompositions, genetic EFA models, and, finally, GRM-SEM multi-dimensional and bi-factor models (**Figure 1**, **Table 1**, **Supplementary Table 4**, **Methods**, **Supplementary Note 3**). For the latter two model types, we adopted a hybrid Independent Pathway / Cholesky (IPC) design that has shown a superior fit in previous analyses (16), as the residual part of the data is always fitted to a saturated (Cholesky) model (**Methods**).

For all phenotypic sets with unambiguously identified numbers of genetic factors ($S_{DLD}$, $S_{LL}$ and $S_{ALL}$), genomic structures were predicted with genetic EFA. Here, we fitted orthogonal (varimax) genetic EFA throughout, given modest genetic factor correlations (**Supplementary Note 2**, **Supplementary Tables 5-6**). Based on the identified best-fitting GRM-SEM models for

$S_{DLD}$ and $S_{LL}$ (**Table 1**, **Supplementary Table 4**, **Figure 3A-F**, **Supplementary Tables 7-8**, **Supplementary Figure 6-7**), we, eventually, added phenotypes to a combined set $S_{ALL}$. To reduce the computational burden, we selected $S_{DLD}$ and $S_{LL}$ measures with both the most substantial factor ($|\lambda|>0.3$) and cross-factor loadings ($|\lambda|>0.1$), representing all phenotypic domains (**Supplementary Table 3**, **Supplementary Note 2**). For the $S_{CRL}$ subset, eigenvalue decomposition did not reveal an exact factor dimension (**Supplementary Figure 8**) and, therefore, the entire set was added to $S_{ALL}$ (**Supplementary Note 2**). Once $S_{ALL}$ building was completed, we repeated the modelling process as described above.

For each modelled phenotype set, $S_{DLD}$ (**Figure 3A-C**, **Supplementary Table 7**, **Supplementary Figure 6**), $S_{LL}$ (**Figure 3D-F**, **Supplementary Table 8**, **Supplementary Figure 7**) and $S_{ALL}$ (**Figure 3G-I**, **Supplementary Table 9**, **Supplementary Figure 9**), a multi-dimensional IPC model fitted the data best (**Table 1**, **Supplementary Table 4**), matching predicted eigenvalues. Model comparisons were based on Akaike and Bayesian information criteria (AIC and BIC), and likelihood ratio tests (LRTs), and the fit of all identified models was highly comparable to a saturated model ($p_{LRT}$=1; **Table 1**, **Supplementary Table 4**). Across subsets ($S_{DLD}$ and $S_{LL}$) and the combined set ($S_{ALL}$), we found stable genetic dimensions (**Figure 3**, **Supplementary Tables 7-8**, **Supplementary Figures 6-7,9**, **Supplementary Note 2**) demonstrating the robustness of underlying genetic structures.

The combined set ($S_{ALL}$), comprised two language phenotypes (language disorder, language level), oppositional defiant disorder (ODD) as a form of general behavioural problems, two developmental milestones (age of self-feeding, age of crawling), control during movement as a proxy for Developmental Coordination Disorder Questionnaire (DCDQ) motor scores and two Repetitive Behaviour Scale-Revised (RBSR) behaviour scores (self-injurious behaviour, sameness behaviour) (**Figure 3H-I**). A three-factor IPC model fitted the data best (**Figure 3G-I**, **Table 1**, **Supplementary Table 4**). The three identified factors captured most strongly language ($A_{lang}$), developmental delay ($A_{dev}$) and behavioural problems ($A_{beh}$) (**Figure 3H**, **Supplementary Figure 9**, **Supplementary Table 9**), consistent with $S_{DLD}$ and $S_{LL}$ models (**Figure 3B,3E**). To explore the factor structure, we focused on standardised genetic factor loadings with an explanatory value of $|\lambda|\geq0.3$ (21), accounting for ~10% phenotypic or liability variation, as well as the factorial coheritability ($f^2_g$), i.e. the fraction of $h^2_{SNP}$ that is explained by a factor.

The first genetic factor captured better language performance, $A_{lang}$ (**Figure 3H**) and was most strongly related to better language level ($\lambda_{lang}$= 0.46, SE=0.08), lower liability to language

disorder ($\lambda_{lang}$=-0.35, SE=0.09) and earlier age of self-feeding ($\lambda_{lang}$=-0.38, SE=0.14). Across phenotypes, this factor accounted for at least half of the trait $h^2_{SNP}$ estimates ($f^2_g$, 0.50-1.00, **Supplementary Table 9**). Notably, this factor also uncovered inverse correlations between children's language ability (e.g. language level) and the age of self-feeding (GRM-SEM $r_g$=-0.71, SE=0.25, **Figure 4A**, **Supplementary Figure 9**).

The second genetic factor, $A_{dev}$, reflecting developmental delay, captured a later age of crawling ($\lambda_{dev}$=0.47, SE=0.10), less motor control (DCDQ control during movement, $\lambda_{dev}$=-0.33, SE=0.13) and more RBSR self-injurious behaviour ($\lambda_{dev}$=0.36, SE=0.10), explaining a considerable proportion of genetic variance ($f^2_g$=0.44-0.84, **Supplementary Table 9**). The third genetic factor, $A_{beh}$, was linked to behaviour problems, almost fully explaining the $h^2_{SNP}$ of each trait ($f^2_g$=1), including RBSR sameness behaviour ($\lambda_{beh}$=0.38, SE=0.12) and liability to ODD ($\lambda_{beh}$=0.45, SE=0.09).

Identified genetic factors largely matched corresponding phenotypic dimensions. Each phenotype had a single meaningful factor loading ($|\lambda|$>0.3) for one factor only (21). However, for liability to language disorder, cross-loadings ($p$<0.05) with all three factors were detected ($\lambda_{lang}$=-0.35, SE=0.09; $\lambda_{dev}$=-0.20, SE=0.10; $\lambda_{beh}$=-0.20, SE=0.10), indicating genetic heterogeneity. Given the broad phenotypic definition of developmental language delay and disorder, genetic links across independent genetic dimensions may arise due to multiple underlying conditions (22).

Further heterogeneity in genetic links was uncovered for self-injurious behaviour. Despite overall stability in factor structures, RBSR self-injurious behaviour, depending on the studied context, was either genetically related to the language $A_{lang}$ factor ($\lambda_{lang}$=0.38, SE=0.10, **Figure 3E**, $S_{LL}$ model) or the developmental-delay-related $A_{dev}$ factor loading ($\lambda_{dev}$=0.36, SE=0.10, **Figure 3H**, $S_{ALL}$ model). Genetic cross-loadings with two independent common dimensions suggest distinct genetic aetiologies (22), matching different forms of self-injurious behaviour in ASD. While some forms involve stereotyped and repetitive behaviour, co-morbid with ID (23), others show neurotypical patterns (24,25) that facilitate cognitive regulation such as the release of 'high pressure' emotions (24,25). In contrast, there was little evidence for genetic links of self-injurious behaviour with the behavioural-problem's factor (**Figure 3E**,**3H**), matching previously reported distinct phenotypic factor structures (8). Thus, self-injurious actions may, at least partially, be aetiologically distinct from other forms of repetitive behaviour.

Next, we confirmed the independence of predicted genetic factors by conducting bi-factor models, each showing a similar fit ($p_{LRT}$≥0.94, **Table 1**, **Supplementary Figures 10-12**). In addition, we corroborated predicted $r_g$ (**Figure 4**) and $h^2_{SNP}$ patterns (**Supplementary Figure 13**), derived from the best-fitting GRM-SEM model for the $S_{ALL}$ set, through comparisons with corresponding GREML analyses. We observed consistent findings throughout, based on 95% CIs, demonstrating that genetic dimensions and structure of multivariate genetic architectures can be accurately predicted by genetic PCA and EFA analyses (**Figure 3A**,**3D**,**3G**), analogous to methodologies developed for summary statistics (26).

Eventually, to enhance the interpretability of identified genetic structures, we mapped ASD subcategory information and PGS for educational attainment (EA) onto the model structure of the $S_{ALL}$ model in SPARK, while preserving the model fit (**Figure 3H** versus **Figure 5A**,**5D**, **Supplementary Table 4**). ASD subcategory information (DSM-IV-based) can provide a clinical reference guiding the interpretation of identified cognitive genetic dimensions, here capturing genetic liability to Asperger, a form of autism without significant impairments in language and cognitive development (27). In contrast, $PGS_{EA}$ presents a genetic correlate of cognitive functioning (28), but also socio-economic status, including health and longevity (29). Here, once mapped, liability to Asperger was genetically linked to the language genetic factor (**Figure 5A**, $\lambda_{lang}$=0.36, SE=0.15). Genetic correlations between liability to Asperger and language level (**Figure 5C**, GRM-SEM $r_g$=0.90, SE=0.19) were positive, consistent with the absence of language problems in this ASD subcategory (3). In contrast, $PGS_{EA}$ were inversely associated with the behavioural problem factor (**Figure 5D**, $\lambda_{beh}$=-0.16, SE=0.06), conditional on the language/cognitive dimension. Consistently, genetic correlations of $PGS_{EA}$ with behavioural measures such as sameness behaviour were inverse (**Figure 5F**, GRM-SEM $r_g$=-0.16, SE=0.06), strengthening support for previously reported links with repetitive behaviour (9).

Note that low sample numbers and/or low $h^2_{SNP}$ of ASD liability prevented a more comprehensive modelling (**Supplementary Figure 14**).

## Multi-dimensional genetic analyses in simplex ASD

Within stage IV, we attempted to reproduce the best-fitting GRM-SEM model identified in the population-representative SPARK sample ($S_{ALL}$) by studying ASD individuals from SSC simplex families. Matching SSC phenotypes showed little evidence for $h^2_{SNP}$ (**Supplementary Figure 15**), consistent with the smaller sample size. Both motor (DCDQ scores) and self-injurious

behaviour (RBSR) scores had to be excluded from follow-up due to near-zero $h^2_{SNP}$ point estimates. These two measures were replaced with further language/cognition and developmental phenotypes to allow for an empirical identification of three genetic dimensions. The final phenotype subset ($S_{SSC}$) reflected phenotypes studied in SPARK: three language/cognition measures (language disorder, language age level, language level), general behaviour (ODD), three developmental milestones (age of crawling, age of self-feeding, age of walking), and the RBSR repetitive behaviour score (sameness behaviour).

As in SPARK, a three-factor model (**Figure 6**, **Supplementary Table 10**) fitted the data best (**Table 1**, **Supplementary Table 4**), matching predicted eigenvalues. The first genetic factor ($A_{F1}$) accounted for variation in language age level ($\lambda_{F1}$=0.33,SE=0.14; $f^2_g$=0.21,SE=0.16) and age of self-feeding ($\lambda_{F1}$=-0.46,SE=0.19; $f^2_g$=1.00,SE<0.01), corresponding to the $A_{lang}$ factor structure in SPARK (**Figure 3B,3E,3H**, **Figure 6B**). Note, within SPARK, language level (i.e. an individual's everyday language skills) and language age level (i.e. an individual's spoken language for their age level) are strongly correlated (GCTA $r_g$=1.00,SE=0.24) and showed, when modelled together, similar association patterns (e.g. $S_{LL}$ model, **Supplementary Figure 7**). The second genetic factor ($A_{F2}$) described variation across developmental-delay-related phenotypes, with the strongest factor loading for age of walking ($\lambda_{F2}$=0.62,SE=0.14; $f^2_g$=0.93,SE=0.22), comparable to the $A_{dev}$ factor structure in SPARK (**Figure 3E,3H**, **Figure 6B**). The third genetic factor ($A_{F3}$) (**Figure 6B**) explained shared genetic variation ($f^2_g$=0.75-1.00, **Supplementary Table 10**) across language/cognition and repetitive (RBSR sameness) behaviour. The strongest factor loadings were observed for language age level ($\lambda_{F3}$=0.61,SE=0.10), language disorder ($\lambda_{F3}$=-0.51,SE=0.11), language level ($\lambda_{F3}$=0.37,SE=0.07), but also RBSR sameness behaviour ($\lambda_{F3}$=0.51, SE=0.12). This cross-trait genetic dimension in the SSC captured strong positive genetic correlations between language and repetitive behaviour (e.g. language level, RBSR sameness behaviour: GRM-SEM $r_g$=0.97, SE=0.07, **Figure 6D**) that were absent in SPARK (language level, RBSR sameness behaviour: GRM-SEM $r_g$=0, **Supplementary Figure 9**).

## Sensitivity analysis

We carried out several sensitivity analyses. We (1) visually confirmed the similarity in structure between the best-fitting model and the bi-factor model across all analysed subsets ($S_{DLD}$, $S_{LL}$, $S_{ALL}$, $S_{SSC}$) (**Supplementary Table 4**, **Supplementary Figures 10-12,16**). Next, we (2) corroborated the superiority in model fit for all identified GRM-SEM models in SPARK and the SSC by comparing their fit with exploratory GRM-SEM models (**Supplementary Table 4**), such

as one-factor independent pathway and IPC models (**Supplementary Figure 17**). To validate the predictive value of EFA models, we (3) confirmed the interchangeability of EFA methods predicting genetic factors (**Supplementary Tables 5-6**) and (4) found strong correlations between EFA-predicted and GRM-SEM estimated factor loadings (Pearson $r > 0.98$ for all analysed models, **Supplementary Figure 18**). Lastly, we (5) performed proof-of-principle simulations (**Supplementary Note 3**). We demonstrated the robustness of the proposed multi-step genomic covariance modelling approach (**Figure 1**), with little evidence for bias and sufficient 95% CI coverage for estimated factor loadings and derived variance components (**Supplementary Tables 11-14**, **Supplementary Figures 19-20**).

# DISCUSSION

Investigating genomic covariance across a broad spectrum of phenotypes in ASD using SEM-based techniques, this case-only study of two large autism cohorts demonstrates that the common genetic architecture of ASD is multi-dimensional. Here, we identified evidence for at least three independent common genetic dimensions associated with phenotypic heterogeneity in ASD.

For population-representative ASD, as reflected in SPARK, we identified three common genetic factors explaining predominantly variation in language/cognition, developmental delay and behavioural problems, with genetic dimensions essentially matching corresponding phenotypic measurements. For simplex ASD, within the SSC, we uncovered structural similarities supporting the first two factors (i.e. language/cognition and developmental delay), indicating conceptual replication. The major difference across cohorts concerned the genetic relationship between language/cognition and behavioural phenotypes. While genetic factors of language/cognition and behaviour were unrelated in population-representative ASD, the underlying phenotypes were strongly genetically related in simplex ASD and captured by a single dimension. Thus, profound structural differences exist in common genetic influences distinguishing population-representative and simplex ASD manifesting in ascertainment-specific patterns. Our findings strengthen the evidence for common genetic contributions to phenotypic variation in ASD (8,9,12) and offer insight into the underlying multi-dimensional common genetic architecture.

Across both cohorts, we found evidence for an independent language/cognition-related factor, as validated through association with higher liability to Asperger in SPARK. Although language performance is not included as a core symptom of ASD in the DSM-5 anymore, our findings confirm that autistic individuals differ considerably in their language presentation (30). While some children with ASD reach intact structural language skills, others are delayed or never master functional spoken language (30). Here, our analyses uncovered, through identification of the language factor, that genomic covariance between (higher) language level and (earlier) age of self-feeding with a spoon, an important personal-social developmental milestone which typically developing children master at about 15-18 months (31,32). Notably, the genetic influences contributing to the age by which children self-feed with a spoon were distinct from genetic factors underlying other motor developmental achievements, such as crawling, sitting or walking, when studied in SPARK. Infant autonomy in feeding, especially eating with the family, has been related to more advanced child language production and comprehension (33). Especially within SPARK (e.g. $S_{LL}$ model), age of self-feeding with a spoon showed moderate to strong relationships with multiple language-related phenotypes and may present an early marker of cognitive and language development in ASD.

We also found robust evidence for a genetic factor that is related to developmental delay within SPARK and the SSC, explaining genetic variation underlying growth, such as the age of crawling, a developmental milestone children typically master between 9-18 months of age (34). Within SPARK, genetic variation was shared beyond the age of crawling (a proxy of the age of walking and sitting) across DCDQ motor control during movement (a proxy of DCDQ total score and fine motor handwriting), language disorder and RBSR self-injurious behaviour. These findings support the contribution of common genetic influences to variation in motor abilities, beyond association with *de novo* mutations (9), even if not captured by PGS for psychiatric disorders or $PGS_{EA}$ (9). The spectrum of genetically linked developmental phenotypes, furthermore, extends reports of genetic associations between ASD polygenic risk and later age of walking in population-based samples (35).

Genetically mediated relationships between language/cognition phenotypes and behaviour across cohorts were heterogeneous, highlighting ascertainment-specific patterns. Within SPARK, the behavioural genetic dimension was independent of the language/cognitive dimension of influences. The behavioural-problems factor explained liability to ODD and variation in repetitive behaviour, especially RBSR sameness behaviour that is a proxy of RBSR total scores and ritualistic behaviour, but not self-injurious behaviour. We validated this factor through inverse

genetic association with $PGS_{EA}$, extending previous findings (9), independent of the language/cognitive dimension. In other words, educational attainment-related associations with symptom variation in ASD are unlikely to implicate cognitive factors, as captured by common genetic influences. Instead, our findings suggest that behavioural problems within a population-representative case-only ASD sample vary with non-cognitive correlates of socio-economic status. It is also possible that common genetic influences underlying the behavioural genetic dimension may, partially, tag rare variation given positive correlations between $PGS_{EA,}$ and rare variant risk scores (9) in SPARK.

In contrast, within the SSC, we observed substantial genetic overlap between most language-related phenotypes and RBSR sameness behaviour. Simplex ASD, compared to multiplex ASD, is more often related to *de novo* mutations (11,14). Our findings may, therefore, present aetiological differences unique to simplex ASD, consistent with qualitative differences in the common genetic architecture of ASD individuals carrying *de novo* variants (5,6). Alternatively, genetic links between behaviour and language/cognition in the SSC might, to some degree, be a consequence of collider bias (36). Simplex families are recruited following strict ascertainment schemes (18). Collider bias can arise when two measures, such as behaviour and language/cognition, are independently related to a third variable, such as common genetic variation, and that third variable is conditioned upon (36). Here, the preferential ascertainment of simplex families depleted for inherited genetic risk (37), including common variation, may introduce artificial genetic relationships between behaviour and language/cognition. Stratifying SEM-predicted shared genetic factor structures by common, rare and *de novo* genetic architectures will shed further light on the complex links between genetic and phenotypic heterogeneity as part of future studies.

Our study has multiple strengths and limitations. First, we developed a data-driven GRM-SEM approach that utilises directly genotyped genome-wide information and facilitates building accurate multi-dimensional models of genomic covariance without the need for summary statistics. Here, we leverage genetic EFA to predict the genetic structure of the best-fitting GRM-SEM model, which is confirmed through comparison with a saturated model. Second, we demonstrate that the common genetic architecture of ASD is multi-dimensional. Thus, genetic analyses modelling the common genetic architecture of ASD require a sufficiently high number of phenotypes to allow for the empirical identification of these dimensions. Third, GRM-SEM relies on population-based assumptions of genotype distributions (i.e. Hardy-Weinberg equilibrium) and may exclude individuals or genetic variation that do not meet these expectations. Fourth, any

genetic relationships within this study will reflect variation within an ASD case-only cohort. A mapping to external references, such as Asperger or $PGS_{EA}$, can aid the interpretation of genetic factors across different research designs. Fifth, the lack of $h^2_{SNP}$ across phenotypes may not only reflect a lack of power but a lack of genetic heterogeneity across phenotypic variation in cases. Especially, social core phenotypes showed little evidence for $h^2_{SNP}$ possibly reflecting high social deficits across all studied individuals with ASD. Sixth, in this study we used transformed scores to aid model simplicity and the convergence of models. While we cannot exclude bias, given the robustness of sensitivity analyses and the consistency with previous findings, it is unlikely that transformed scores profoundly changed underlying genetic structures. Seventh, our study cannot yet address sex-specific differences in common genetic architectures, as previously reported (9), especially across non-European ancestry backgrounds. Because the prevalence of ASD is higher in males, the sex distribution in both samples is skewed. There is a low representation of females in ASD cohorts, given male preponderance of the condition, that prevents robust modelling using GRM-SEM and our results may, therefore, be less generalisable for females.

Together our results describe phenotypic variation in ASD as complex traits that are, at least partially, genetically linked due to common genetic factors that are augmented by ascertainment-specific patterns. Here, we show that multi-dimensional common genetic architectures can be accurately identified with a data-driven GRM-SEM approach utilising genome-wide genotyping data.

# ONLINE METHODS

## Samples

The SPARK cohort (https://sparkforautism.org/) (17) is a nationwide autism study across the US including simplex and multiplex families. Here, we studied SPARK phenotype (version 3) and genome-wide (version November 2018) data. This data freeze includes 59,218 individuals between ages 1 and 85, who received a professional diagnosis of ASD/autism (85%<18 years; 79% male), their biological parents, and, if available, one unaffected control sibling as well as all affected siblings for multiplex families (21,689 trios (including simplex families); 6,552 multiplex families). Written informed consent was completed by the parent or legal guardian of the children participating in the study.

The SSC cohort (https://www.sfari.org/resource/simons-simplex-collection/) (18) is a US collection of simplex families. Here, we investigated phenotype (version 15.3) and genome-wide (whole-genome 2 data release) data. This data freeze represents 2,591 affected children aged 4 to 17 years 11 months, including 2,643 simplex families with one (and only one) child with ASD and their unaffected biological parents and unaffected siblings. Informed consent and assent were provided for all participants.

We received ethical approval to access and analyse pre-collected de-identified genotype and phenotype data from these cohorts from the Radboud University Ethics Committee Social Science. All analyses were restricted to individuals with ASD with phenotypic and genetic information.

## Genotype information

*SPARK.* Genome-wide genotypes were obtained with the Infinium Global Screening Array-24 v.1.0. After individual and variant quality control (QC), 5,331 unrelated individuals (79.85% males, median age: 9 years) of European ancestry diagnosed with ASD, with genetic and phenotype information (see below) were included in the study (**Supplementary Methods 1**, **Supplementary Figure 1**). Individuals were excluded due to confirmed genetic syndromes/conditions, birth complications (i.e. birth defects, foetal alcohol syndrome, bleeding into the brain, insufficient oxygen at birth), other cognitive impairments or a brain injury (i.e. brain infection, lead poisoning, traumatic brain injury), similar to SSC exclusion criteria (see below). A genetic relationship matrix (GRM) (19) based on directly genotyped markers ($N_{SNPs}$=450,491) was created in PLINK (v1.9) (38), applying a relationship cut-off of 0.05.

*SSC*. We used genome-wide data from three arrays: Illumina Human1M v1.0, Illumina Human1M-Duov3 and Illumina HumanOmni2.5. For each array, individual and variant QC were performed separately (see **Supplementary Methods 2**). Subsequently, genotype data were merged across the three arrays and again subjected to individual and variant-based QC (**Supplementary Methods 2**). After QC, 1,946 unrelated individuals (86.33% males, median age: 9 years) of European ancestry diagnosed with ASD with genetic and ASD phenotype information were included in the study (**Supplementary Figure 2**). Individuals were excluded according to SSC exclusion criteria, such as premature birth, brain injury/damage/abnormality, prenatal/birth complications, confirmed genetic syndromes/conditions, severe sensory/motor difficulties or

412 nutritional/psychological deprivation. A GRM (19) based on directly genotyped markers
413 ($N_{SNPs}$=457,961) was created in PLINK (v1.9) (38), applying a relationship cut-off of 0.05.

414 ## Phenotypes

415 *SPARK*. We studied parent-reported measures of ASD phenotypes and co-morbid
416 disorders/disabilities spanning the domains of language and cognition (9 measures), general
417 behaviour (9 measures), repetitive behaviour (7 measures), social (2 measures) and motor
418 abilities (6 measures), as well as affective disorders (3 measures) and developmental milestones
419 (11 measures). Phenotypes were extracted from the Basic Medical Screening Questionnaire
420 (BMS), the Social Communication Questionnaire-Lifetime (SCQ) (39), the SPARK Background
421 History Questionnaire (BGHX), the Repetitive Behaviours Scale-Revised (RBSR) (40), and the
422 Developmental Coordination Disorder Questionnaire (DCDQ) (41), including 47 out of 149
423 available SPARK phenotypes (**Supplementary Methods 1, Supplementary Figure 1,**
424 **Supplementary Table 1**).

425 The selected phenotypes included 21 categorical (within-sample prevalence of 5%) and
426 26 continuous phenotypes. At least 2,910 autistic individuals had phenotype and genotype data
427 per trait (**Supplementary Table 1**). Among all the studied individuals in the SPARK sample,
428 information on ASD subcategories was available for 1,754 individuals only: Asperger ($N_{ind}$=716,
429 79.05% males, age range: 2-60 years), childhood autism ($N_{ind}$=624, 81.57% males, age range: 1-
430 55 years) and Pervasive Developmental Disorder Not Otherwise Specified (PDD-NOS, $N_{ind}$=414,
431 males=80.67% males, age range: 2-45 years). Consequently, we did not include ASD
432 subcategory information directly within our modelling approach but instead mapped it onto the
433 best-fitting model (reference Asperger=1, childhood autism=0, PDD-NOS=0, non-subcategory
434 data= NA, deviance-transformed, see below).

435 *SSC*. We studied parent-reported measures of language and cognition (5 measures),
436 general behaviour (1 measure), repetitive behaviour (4 measures), and motor abilities (3
437 measures), as well as developmental milestones (4 measures). These were comparable to
438 SPARK measures, for follow-up analyses. Phenotypes were selected from the SSC BGHX, the
439 SSC Diagnosis Summary Form, the SSC Medical History Interview, RBSR (40), DCDQ (41), the
440 Child Behavior Checklist (CBCL 6-18) (42), and the Autism Diagnostic Observation Scale (ADOS)
441 (43) (**Supplementary Figure 2, Supplementary Table 2**).

442 ## Phenotype transformations

Continuous scores were transformed with ordinary least square regression and categorical scores with logistic regression [R:stats package]. Before transformation, all phenotypes were adjusted for sex, age, age squared, and ten ancestry-informative principal components (44), where the latter correct for subtle ancestry differences among individuals of Caucasian ancestry. For continuous phenotypes, residuals were rank-transformed and regressed again on covariates to achieve normality of transformed scores without a re-introduction of covariate effects (fully-adjusted two-stage rank normalisation)(45). For categorical phenotypes and co-morbid disorders, we constructed deviance residuals as the difference between the logistic model fit and the fit of an ideal model. Deviance residuals approximate the liability as observed within an ASD-only sample (henceforth referred to as liability), given that SPARK is a population-representative sample of ASD individuals, and there is no over-sampling of ASD cases with specific co-morbid disorders or phenotypes. For the SSC, liability is approximated for a simplex ASD case-only sample. We carried out extensive sensitivity analyses to ensure the validity of the transformed scores. For this purpose, we compared $h^2_{SNP}$ estimations (**Supplementary Figure 3**) and phenotypic correlation analyses for untransformed and transformed scores (**Supplementary Figure 21**). Pertinent to this work, analyses were conducted with transformed scores to ease the modelling process, i.e. rank-transformed scores for continuous phenotypes and deviance residuals for categorical phenotypes.

## Univariate and bivariate genetic variance analyses

Univariate ($h^2_{SNP}$) analyses, reflecting, here, the proportion of phenotypic variance among autistic individuals as explained by genotyped variants (SNPs), were carried out with GREML, as implemented in Genome-wide Complex Trait Analysis (GCTA, v1.93.0) software (19). GRMs were constructed from genome-wide genotyping information (see **Supplementary Methods 1-2**).

Bivariate genetic correlations ($r_g$) across phenotypes were estimated using bivariate GREML (20). Genetic correlations reflect the extent to which the same genetic factors influence two measures.

## Multivariate modelling of genomic covariance

We modelled the multivariate genetic variance structure of ASD phenotypes using GRM-SEM as implemented in R:grmsem (v1.1.2, https://gitlab.gwdg.de/beate.stpourcain/grmsem) previously known as *gsem* (15,16).

GRM-SEM applies structural equation modelling techniques to analyse genomic covariance in samples of unrelated individuals using a maximum likelihood approach (15). We define the expected phenotypic variance, $\Sigma_V$, of a multivariate normal phenotype Y (for 1...k traits) where $Y_i \sim N_k (\mu, \Sigma_V)$, as the sum of the expected genetic and residual variance components, $\Sigma_A$ and $\Sigma_E$:

$$\Sigma_V = \Sigma_A + \Sigma_E \quad (1)$$

where $\Sigma_V$, $\Sigma_A$ and $\Sigma_E$ are symmetric k x k matrices. The residual variance component, potentially, includes environmental factors, random error, non-additive genetic variance, rare variance or any other genetic influence not captured by the GRM (15,16,19). Within GRM-SEM, genetic and environmental influences are modelled as latent variables. The phenotypic variance for each measure Y can be dissected into genetic and residual influences (AE model), analogous to twin research (46):

$$\Sigma_V = \Lambda_A \Psi_A \Lambda_A^T \otimes G + \Lambda_E \Psi_E \Lambda_E^T \otimes I \quad (2)$$

where $\Lambda_A$ and $\Lambda_E$ are matrices of genetic and residual factor loadings with dimensions k x p, where p is the number of factor loadings. $\Psi_A$ and $\Psi_E$ are p x p matrices of genetic and residual factor variances, respectively. G is a n x n GRM matrix for all pairs of n independent individuals (19) constructed from the variants presented on a genome-wide genotyping chip, and I is a n x n identity matrix. The symbol $\otimes$ denotes the Kronecker product. In this work, $\Psi_A$ and $\Psi_E$ have been restricted to an identity matrix, given modest genetic correlations between latent variables, as predicted by oblique genetic EFA. Bi-factor models confirmed the independence of factor structures (see below). Note that we assume besides structured genetic covariance also structured residual covariance that can contribute to phenotypic covariance patterns (16). We analyse, here, a proportion of genetic variance in ASD individuals that can be modelled according to population-based principles.

We fitted the following multivariate models (15,16):

i. *Cholesky model*: The Cholesky decomposition model (**Supplementary Figure 17A**) is a saturated i.e. fully parametrised descriptive model without any restrictions on the structure of latent genetic and residual influences. This model is fitted to the data through the decomposition of both the genetic variance and residual variance into as many latent variables (factors) as there are observed variables. Here, $\Lambda_A$ and $\Lambda_E$ are k

x k lower diagonal matrices. Note that other saturated models, such as direct symmetric models (47), were not fitted due to convergence problems with multicollinear data (not shown). Cholesky-derived genetic trait correlations provided input data to estimate the dimensionality of shared genetic factors ($n_{AC}$) using genetic PCA (see below). The Cholesky-derived genetic trait covariance was used as input to predict the genomic covariance structure of the best-fitting model, with genetic EFA (see below).

ii. *Independent pathway model*: The independent pathway model (**Supplementary Figure 17B**) specifies one or more shared genetic and one or more shared residual factors, where $n_{AC}$ is the number of shared genetic factors and $n_{EC}$ is the number of residual factors, in addition to trait-specific genetic and residual influences, one for each trait. $\Lambda_A$ and $\Lambda_E$ have the dimensions k x $p_a$ and k x $p_e$, respectively, where $p_a$ is the sum of $n_{AC}$ and k, and $p_e$ is the sum of $n_{EC}$ + k. Pertinent to this study, we fitted 1-factor models only ($n_{AC} = n_{EC} = 1$).

iii. *Hybrid Independent Pathway/Cholesky model (IPC)*. The IPC model (**Supplementary Figure 17C**) structures the genetic variance as an independent pathway model (consisting of shared and measurement-specific influences where $\Lambda_A$ has a dimension of $k(n_{AC}+k)$) and the residual variance as a Cholesky model (where $\Lambda_E$ is a lower diagonal k x k matrix). Here, we fitted 1-factor ($n_{AC}=1$; $k_{traits}\geq 3$) and multi-factor ($n_{AC}=2$, $k\geq 6$; $n_{AC}=3$; $k\geq 8$) IPC models, such that for the latter $N_{\Lambda(EFA)}<N_{\Lambda(saturated)}$. The genetic part of multi-factor IPC models was informed by the estimated number of genetic factors $n_{AC}$ using proxy genetic PCA and the estimated factor loadings from genetic EFA (see below). Specifically, we used EFA-predicted information to define starting values and constraints (i.e. setting EFA factor loadings $|\lambda|<0.1$ in the corresponding genetic part of the GRM-SEM model to zero). As a rule of thumb, zero loadings have been defined as factor loading scores between -.10 and +.10 (48). Once fitted, we further trimmed the model by removing specific genetic factor loadings near zero (GRM-SEM factor loadings $|\lambda|<0.01$). The residual part of the model remained unchanged and was fitted as a Cholesky model.

To confirm the independence of shared genetic factors for the best-fitting multi-factor IPC model, we fitted a bi-factor model of genetic variance within the IPC framework. The bi-factor model (49) consists of a general factor and one or more grouping factors, where each trait loads on the general factor, assuming statistical

independence between these latent genetic dimensions. Given the bi-factor parametrisation, the model benefits from rotational invariance and unlimited dimensionality (50).

The goodness-of-fit for each model was evaluated with likelihood ratio tests (LRTs), Akaike information criterion (AIC) and the Bayesian information criterion (BIC) (51). Evidence for GRM-SEM factor loadings was assessed using Wald tests, based on unstandardized scores, while reported coefficients λ represent standardised factor loadings (setting the phenotypic variance to unit variance).

For the best-fitting models, we estimated heritability ($h^2_{SNP}$), genetic correlations ($r_g$), and factorial co-heritabilities ($f^2_g$, i.e. the proportion of total trait genetic variance explained by a specific genetic factor). We defined bivariate genetic correlation between phenotypes, measuring the extent to which two phenotypes share genetic factors (ranging from -1 to 1 (52) according to:

$$r_g = \frac{\sigma_{g12}}{\sqrt{\sigma^2_{g1}\sigma^2_{g2}}} \quad (3)$$

where $\sigma_{g12}$ is the genetic covariance between two phenotypes 1 and 2, and $\sigma^2_{g1}$ and $\sigma^2_{g2}$ are the respective genetic variances. In addition, we estimate the factorial co-heritability $f_g^2$ as the relative contribution of a genetic factor to the genetic variance of a phenotype, defined as:

$$f_g^2 = \frac{\sigma^2_{g_{it}}}{\sum \sigma^2_{g_{it}}} = \frac{\sigma^2_{g_{it}}}{\sigma^2_{g_t}} \quad (4)$$

where $\sigma^2_{g\_it}$ is the genetic variance of the genetic factor *i* contributing to trait t and $\sigma^2_{g\_t}$ the total genetic variance of trait t, based on standardised factor loadings. Corresponding SEs were derived using the Delta method.

*Phenotype selection.* For GRM-SEM, we studied transformed phenotypes (see above) in combination with GRMs constructed from genotyped genome-wide variants in unrelated ASD individuals of European descent. GRM-SEM models are computationally expensive (15). For example, an 8-factor Cholesky decomposition model, as fitted within this study, can require up to 6 weeks of computing time even on a system incorporating at least four parallel cores of 3 GHz, and requiring up to 40 Gb (max vmem) memory. Hence, we streamlined the modelling process by combining measures of the same questionnaire (i.e. BGHX, DCDQ and RBSR) that shared an underlying genetic architecture (GRM-SEM $r_g$=1). We only retained measures with the highest

genetic correlations to (a) limit the number of studied phenotypes using proxy measures and (b) aid model convergence by reducing collinearity.

## Eigenvalue decomposition of genetic correlations: genetic PCA

The dimensionality of shared genetic factors ($n_{AC}$) across a set of phenotypes was estimated by the spectral decomposition (53) [R:base package]. For the estimation, we used a Cholesky-derived genetic correlation matrix. Eigenvalues of this genetic PCA were plotted as a scree plot. The number of factors was estimated with the Optimal Coordinate criterion [R:nFactors package](54), applying a joint Kaiser's rule (eigenvalue > 1) (55,56) and Cattell's scree test (57).

## Exploratory factor analysis of genetic covariance: genetic EFA

Given evidence for multiple genetic factors (dimensionality of shared genetic factors $n_{AC}$>1), we carried out for each set of selected phenotypes a genetic EFA (58) predicting underlying genetic factor structures, using *lavaan* (59) [R:lavaan package] software. As genetic trait covariance is not directly observable, we analysed the predicted genetic covariance matrix derived from a saturated (Cholesky) GRM-SEM model (see above). Factor solutions were estimated using a Diagonally Weighted Least Squares (DWLS) algorithm (60), i.e. a robust Weighted Least Squares (WLS) method that can be applied to skewed data where the likelihood function for any parameter θ is given as

$$l(\theta) = \frac{1}{2} tr[(S - \Sigma(\theta))\mathrm{W}^{-1}] \quad (5)$$

where S is the observed (here Cholesky predicted genetic covariance matrix) and Σ the EFA model-implied genetic covariance matrix. Inverse weighting was carried out with a diagonal weight matrix W, based on the estimated variance $\tilde{V}$ of the genetic covariance $V_A$, as derived with a Cholesky model, where W = diag($\tilde{V}(V_A)$). For comparison, we also carried out an unweighted least square estimation, where the identity matrix replaces W. Factors in *lavaan* were rotated using either orthogonal or oblique rotation techniques, performing EFA varimax and oblimin, respectively. We opted for an EFA varimax model if the predicted genetic correlation between genetic factors by an EFA oblimin model was modest (i.e. $r \leq 0.32$ (21) and thus ignorable) or if the EFA oblimin model produced a similar pattern of loadings as EFA varimax (21). In other words, the EFA oblimin solution did not increase the simplicity of the model (21). The factor loadings of the selected EFA model were utilised to define starting values and constraints of GRM-SEM multi-

593 factor IPC models, setting genetic EFA factor loadings |λ|<0.1 in the corresponding genetic part
594 of the GRM-SEM model to zero (21).

595 Note that an evaluation of EFA models based on model fit criteria established in
596 observational research is not meaningful here, as the studied genetic covariance matrix
597 (Cholesky) is estimated with an error that may result in negative uniqueness of the predicted
598 genetic variance, violating modelling assumptions (known as a Heywood case) (61).

599 For sensitivity analyses, we also compared estimates of EFA *lavaan* with estimates of
600 other EFA software such as *fa* [R:psych package] which does not allow for inverse weighting (62).

601 ## Simulation study

602 To evaluate the robustness of the proposed multi-step genomic covariance modelling
603 approach, and in particular to assess bias, we carried out simulations comparing true values with
604 GRM-SEM IPC factor loadings, but also EFA-predicted factor loadings (**Supplementary Tables**
605 **11-14, Supplementary Figures 19-20**), as described in detail in the supplement
606 (**Supplementary Note 3**).

607 In brief, assuming multivariate normality, we simulated six-variate traits with either two
608 shared genetic factors without correlation or two shared genetic factors with cross-loading as
609 detailed by path models in **Supplementary Figures 19 and 20**, respectively, across 20 replicates.
610 Each six-variate trait was based on Z-standardized phenotypes with 2,000 individuals per
611 phenotype and (for simplicity) 5,000 causal loci, to increase power. Besides the median estimate,
612 simulation performance measures included the median bias, the median empirical standard error
613 (empSE) and coverage of 95%-confidence intervals (such that the estimated 95%-confidence
614 interval contains the true value), and the respective Monte-Carlo SEs (MCSE).

615 ## Multiple testing

616 A correction for multiple testing of estimated GRM-SEM factor loadings of our analysis is
617 not directly applicable. We jointly analyse multiple phenotypes using a multivariate approach to
618 comprehensively represent all shared genetic factors across the studied phenotypic spectrum.
619 $h^2_{SNP}$ and $r_g$ estimates from a GCTA screen within Stage I are not individually interpreted, given
620 the preliminary character of these analyses. However, if a multiple testing adjustment for
621 individual measures reported during Stage I were considered, an experiment-wide threshold of

622 $p$<0.0015 (0.05/34 independent measures) would be needed to be applied, as estimated with
623 Matrix Spectral Decomposition (matSpD) (63), based on phenotypic score correlations.

624 ## Univariate polygenic scoring analysis in SPARK

625 Consistent with current guidelines (64), we constructed PGS for EA within SPARK based
626 on high-quality genome-wide imputed SNPs (**Supplementary Methods 3**), utilising available
627 summary statistics from recent EA meta-GWAS (65). For this purpose, we used PRS-CS software
628 (66), which applies continuous-shrinkage parameter to adjust SNP effect sizes for linkage
629 disequilibrium. Once SNP effect sizes were calculated in PRS-CS, $PGS_{EA}$ scores were calculated
630 in PLINK (38) and, subsequently, Z-standardised.

# TABLES

**Table 1. Model fit comparison.**

| Model | Type | log-likelihood | $N_{par}$ | AIC | BIC | $LRT_{Cholesky}$ | | $LRT_{Bi\text{-}factor}$ | |
|---|---|---|---|---|---|---|---|---|---|
| | | | | | | $\Delta\chi^2(\Delta df)$ | *p* | $\Delta\chi^2(\Delta df)$ | *p* |
| **SPARK** | | | | | | | | | |
| $S_{DLD}$ model: $N_{traits}$=7, $N_{ind}$=5279 | | | | | | | | | |
| Cholesky | saturated | -13343.57 | 56 | 26799.13 | 27167.14 | - | | - | |
| Bi-factor | two-factor | -13345.64 | 46 | 26783.28 | 27085.56 | 4.14(10) | 0.94 | - | |
| IPC best-fit | two-factor | -13345.66 | 40 | **26771.33** | **27034.19** | 4.19(16) | 1.00 | 0.05(6) | 1.00 |
| $S_{LL}$ *model:* $N_{traits}$=7, $N_{ind}$=5279 | | | | | | | | | |
| Cholesky | saturated | -12524.86 | 56 | 25161.72 | 25529.72 | - | | - | |
| Bi-factor | two-factor | -12526.61 | 46 | 25145.23 | 25447.51 | 3.51(10) | 0.97 | - | |
| IPC best-fit | two-factor | -12527.13 | 41 | **25136.27** | **25405.70** | 4.55(15) | 1.00 | 1.04(5) | 0.96 |
| $S_{ALL}$ ($S_{DLD}$, $S_{LL}$ and $S_{CRL}$) *model:* $N_{traits}$=8, $N_{ind}$=5279 | | | | | | | | | |
| Cholesky | saturated | -15248.61 | 72 | 30641.23 | 31114.37 | - | | - | |
| Bi-factor | three-factor | -15249.97 | 62 | 30623.94 | 31031.37 | 2.71(10) | 0.99 | - | |
| IPC best-fit | three-factor | -15250.96 | 53 | **30607.92** | **30956.21** | 4.69(19) | 1.00 | 1.98(9) | 0.99 |
| **SSC** | | | | | | | | | |
| $S_{ALL}$ *model:* $N_{traits}$=8, $N_{ind}$=1940 | | | | | | | | | |
| Cholesky | saturated | -6342.50 | 72 | 12828.99 | 13230.07 | - | | - | |
| Bi-factor | three-factor | -6342.59 | 63 | 12811.18 | 13162.12 | 0.19(9) | 1.00 | - | |
| IPC best-fit | three-factor | -6342.60 | 53 | **12791.19** | **13086.43** | 0.20(19) | 1.00 | 0.01(10) | 1.00 |

The genomic covariance structure across SPARK and SSC phenotype sets were modelled using saturated, bi-factor and multi-factor GRM-SEM IPC models (additional comparisons with one-factor IPC models are shown in Supplementary Table 4). The fit across models was compared with likelihood ratio tests (LRT), AIC and BIC for the phenotype subsets: $S_{DLD}$, $S_{LL}$, $S_{ALL}$(combined subset: $S_{DLD}$, $S_{LL}$, $S_{CRL}$) and $S_{SSC}$. The lowest AIC and BIC values are shown in bold.

*Abbreviations*: AIC (Akaike information criterion); BIC (Bayesian information criterion); IPC (Hybrid Independent Pathway (genetic part) / Cholesky (residual part) model); $N_{par}$ (number of parameters), $S_{CRL}$ (age of crawling subset), $S_{DLD}$ (language disorder subset), $S_{LL}$ (language level subset), and $S_{SSC}$ (follow-up subset).

# FIGURES

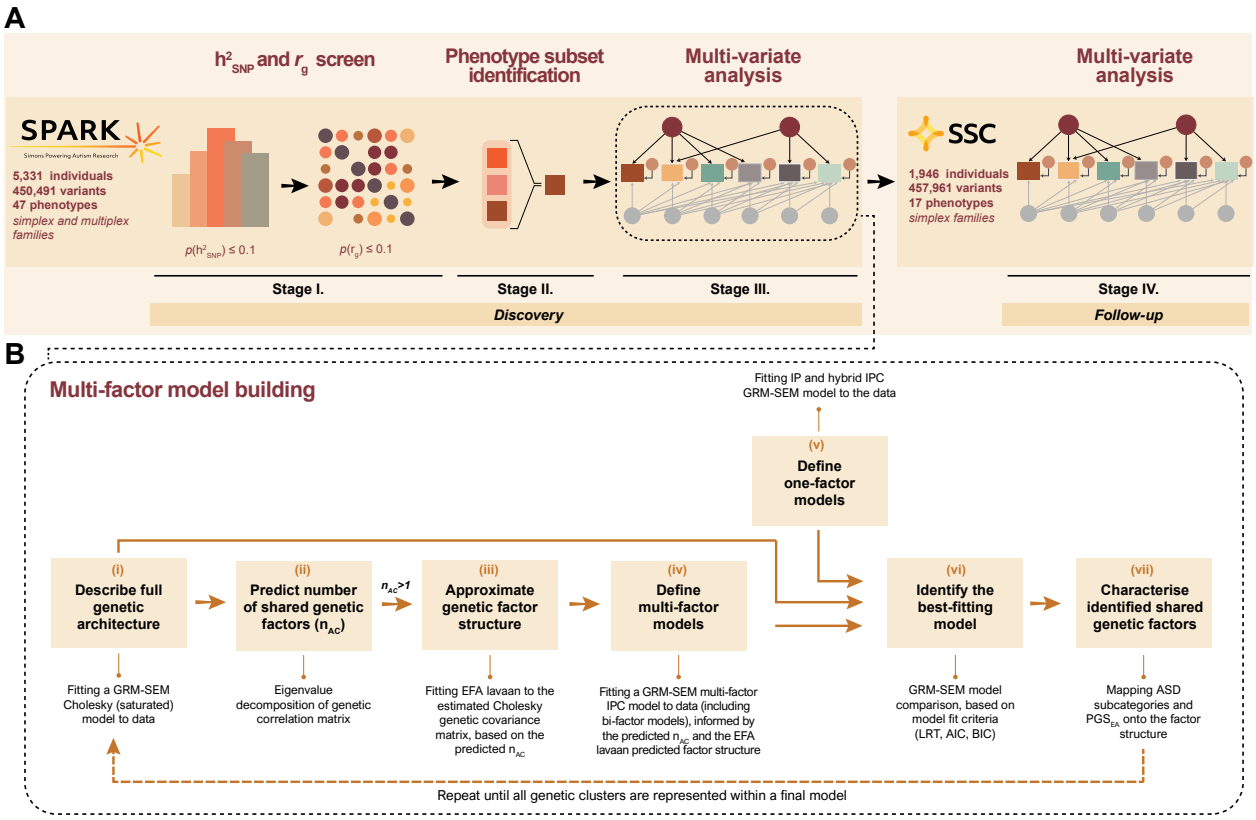


**Figure 1. Workflow of the study. (A)** Multivariate discovery analyses were carried out in the Simons Powering Autism Research (SPARK) sample (Stages I-III) and the best-fitting final SPARK multi-factor model was followed-up in the Simons Simplex Collection (SSC, Stage IV). **(B)** Data-driven approach to model genomic covariance with genetic-relationship-matrix structural equation modelling (GRM-SEM). We fitted (i) a saturated GRM-SEM (Cholesky) model to describe the genetic architecture. Based on this information, we (ii) predicted the number of shared genetic factors ($n_{AC}$) across phenotypes through eigenvalue decomposition of Cholesky-derived genetic correlations. If $n_{AC}$ >1, we (iii) approximated the underlying genetic factor structure through exploratory factor analysis (EFA) of Cholesky-derived genetic trait covariance. We used this information on genetic factor structures from (ii) and (iii) to fit (iv) multi-factor Independent Pathway/Cholesky (IPC) models, including bi-factor models (to confirm the independence of shared genetic factors). For comparison only, we fitted (v) one-factor Independent Pathway (IP) and IPC models, analogous to twin analyses. We compared (vi) the model fit of multi-factor models to one-factor models and the saturated model to identify the best-fitting model. This multi-step approach was repeated until all phenotype subsets were combined into a final model. Eventually, we (vii) characterised the factor structure of the final best-fitting model by mapping it

661 to a clinical reference (DSM-IV-based ASD subcategories) and to the polygenic score for
662 educational attainment ($PGS_{EA}$), enhancing the interpretability of predicted factor structures.

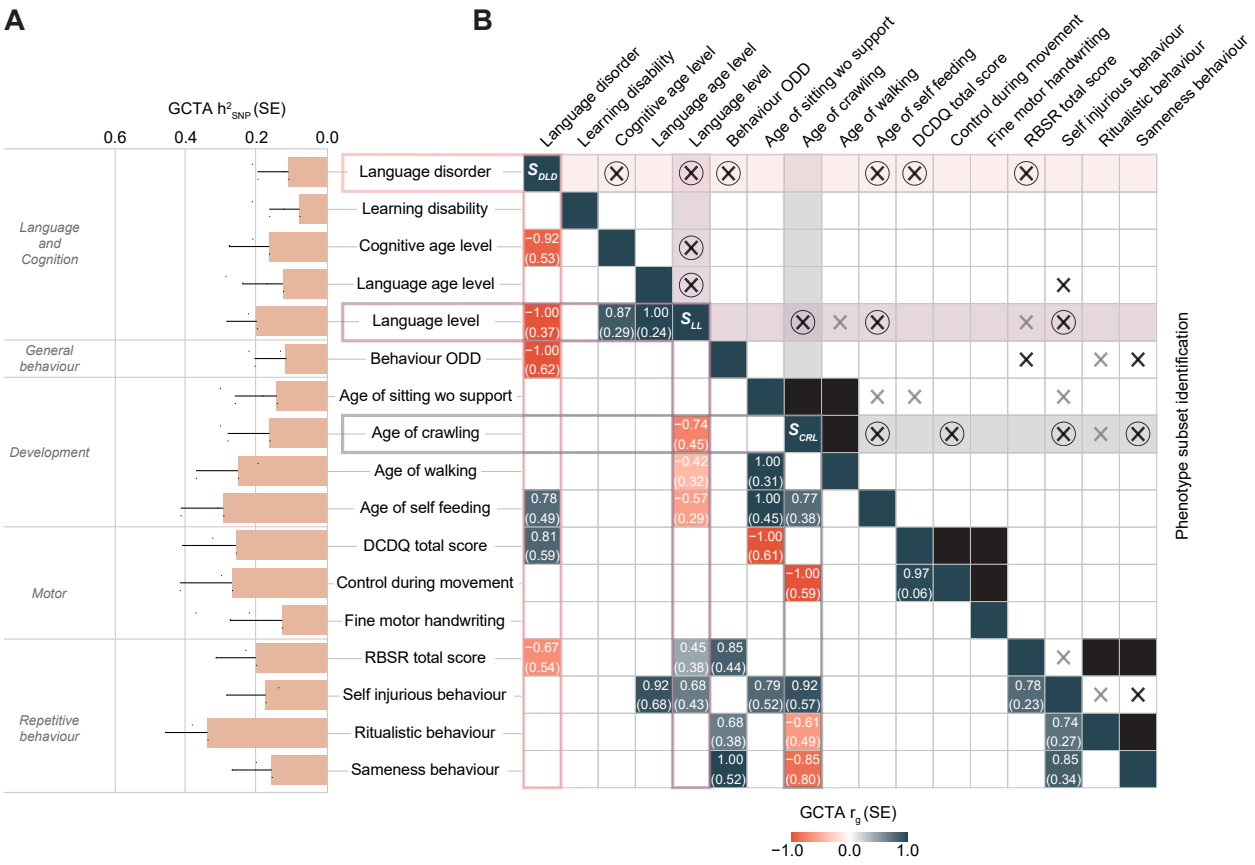


**Figure 2. Screen for heritable and genetically interrelated phenotypes in SPARK. (A)** Heritability ($h^2_{SNP}$) of continuous and categorical ASD phenotypes (p≤0.1) as estimated by GCTA. A complete figure of all analysed phenotypes is shown in Supplementary Figure 3. The error bars represent standard errors. Estimates were based on transformed scores: deviance residuals (for categorical phenotypes) or rank-transformed residuals (for continuous phenotypes). **(B)** The lower triangle shows the genetic correlation screen ($r_g$) across ASD phenotypes as shown in (A), passing p($r_g$)≤0.1, as estimated with GCTA. A complete figure of all correlations is shown in Supplementary Figure 4. The upper triangle shows the selected phenotype subsets that, together, comprehensively capture the genetic correlations (lower triangle) across studied phenotypes. Each phenotypic subset has a 'node' phenotype: $S_{DLD}$ (language disorder), $S_{LL}$ (language level) and $S_{CRL}$ (age of crawling). Phenotypes within a subset are directly genetically correlated with the 'node' phenotype (p≤0.1). The black boxes symbolise proxy phenotypes, as identified within uni-factorial GRM-SEM ($r_g$=1, Supplementary Figure 5). Circled 'x' within shaded boxes indicate the phenotypes that are included in each subset and were directly modelled with GRM-SEM. A black 'x' indicates directly estimated and a grey 'x' indirectly (proxied) genetic relationships. Phenotypes

679 were adjusted for covariates and transformed into either rank-transformed residuals (continuous
680 measures) or deviance residuals (categorical measures).

681 *Abbreviations*: DCDQ (Developmental Coordination Disorder Questionnaire), GCTA (Genome-
682 wide Complex Trait Analysis), GRM-SEM (Genetic Relationship Matrix Structural Equation
683 Modelling), ODD (oppositional defiant disorder), RBSR (Repetitive Behaviour Scale-Revised).

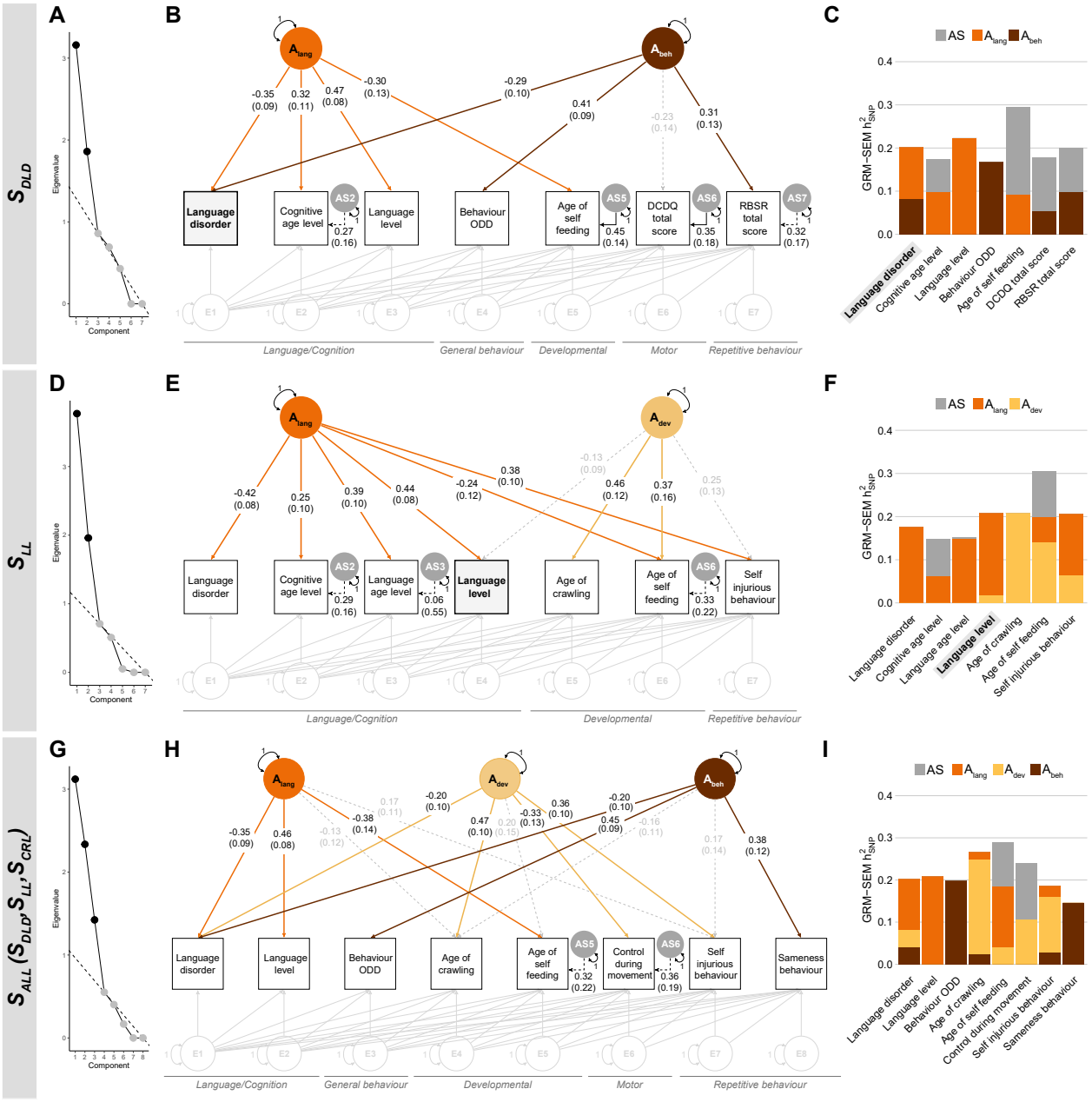


**Figure 3. Multi-factor GRM-SEM models in SPARK. (A)** Scree plot, **(B)** path diagram and **(C)** standardised genetic variance (GRM-SEM $h^2_{SNP}$) plot of the best-fitting GRM-SEM IPC model for the language disorder ($S_{DLD}$) set. **(D)** Scree plot, **(E)** path diagram and **(F)** standardised genetic variance (GRM-SEM $h^2_{SNP}$) plot of the best-fitting GRM-SEM model for the language level ($S_{LL}$) set. **(G)** Scree plot, **(H)** path diagram and **(I)** standardised genetic variance (GRM-SEM $h^2_{SNP}$) plot of the best-fitting GRM-SEM model for the combined ($S_{ALL}$: $S_{DLD}$, $S_{LL}$ and $S_{CRL}$ set) set. **(A,D,G)** Scree plots are based on the eigenvalue decomposition of genetic correlations derived from a GRM-SEM Cholesky model, depicting the number of estimated shared genetic factors (in black) according to the optimal coordinate criterion. The dashed line indicates the "scree" of the plot

(grey). **(B,E,H)** Observed measures are represented by squares and latent variables by circles (A: shared genetic factor, AS: specific genetic factor, E: residual factor). Dotted and solid single-headed arrows (factor loadings) define relationships between variables with $p>0.05$ and $p\leq0.05$, respectively. The genetic part of the model has been modelled using an Independent Pathway model, and the residual part using a Cholesky model (grey). (**C,F,I)** SEs for GRM-SEM $h^2_{SNP}$ contributions have been omitted for clarity. Note that no GRM-SEM model was fitted to the third $S_{CRL}$ (age of crawling) subset, as the number of genetic factors could not be unambiguously predicted by the optimal coordinate criterion.

*Abbreviations*: $A_{lang}$ (Genetic language factor), $A_{dev}$ (Genetic developmental-delay factor), $A_{beh}$ (Genetic behavioural-problems factor), DCDQ (Developmental Coordination Disorder Questionnaire), $h^2_{SNP}$ (Single nucleotide polymorphism-based heritability), IPC (Independent Pathway-Cholesky GRM-SEM model), ODD (Oppositional Defiant Disorder), RBSR (Repetitive Behaviours Scale-Revised).

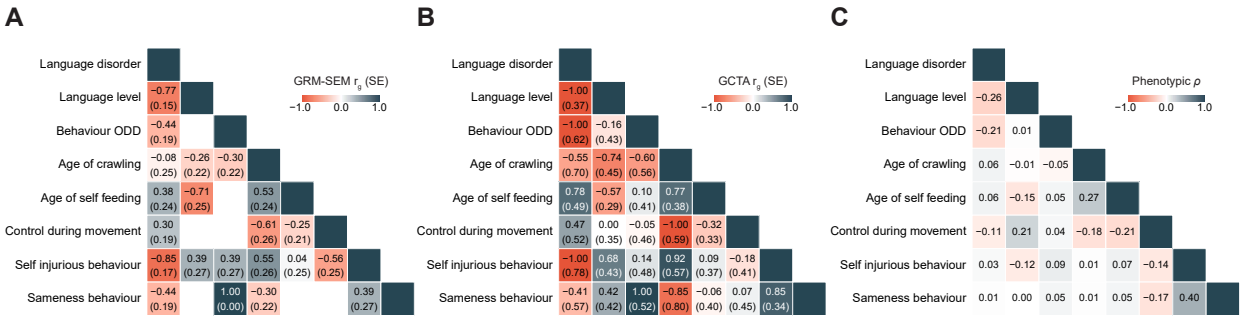


**Figure 4. Correlations for the combined ($S_{ALL}$) phenotypic subset.** Figure shows **(A)** GRM-SEM genetic correlations, **(B)** GCTA genetic correlations and **(C)** Spearman phenotypic correlations. All correlations are based on transformed measures.

*Abbreviations*: GCTA (Genome-wide Complex Trait Analysis), GRM-SEM (Genetic Relationship Matrix Structural Equation Modelling), ODD (oppositional defiant disorder).

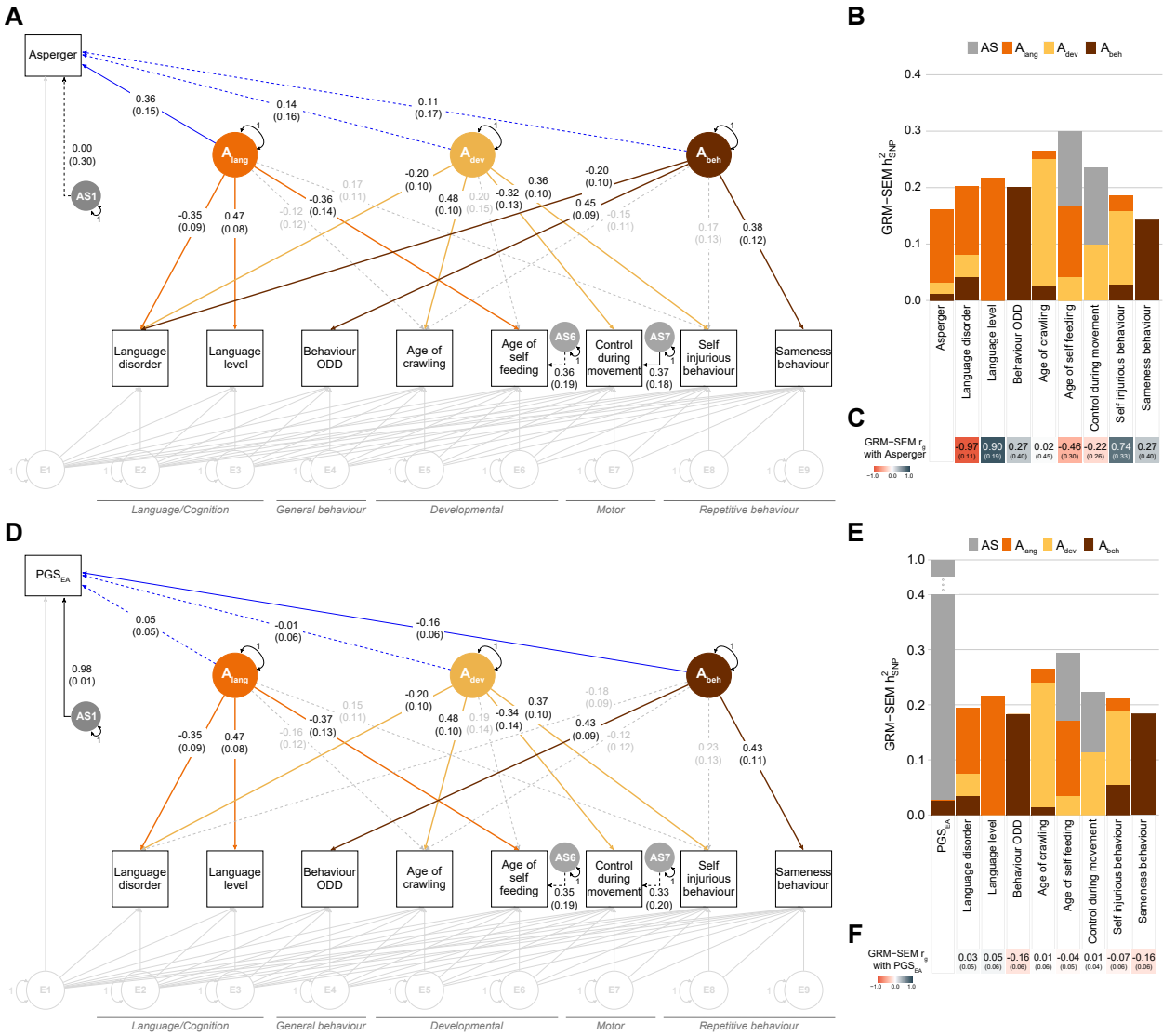


**Figure 5. ASD subcategory mapping of the multi-factor GRM-SEM model for the combined ($S_{ALL}$) set in SPARK. (A)** Path diagram of an extended GRM-SEM IPC model mapping liability to Asperger (reference: Asperger against other ASD subcategories) onto the model structure of the best-fitting ($S_{ALL}$, Figure 3H) SPARK model. **(B)** Corresponding standardised genetic variance (GRM-SEM $h^2_{SNP}$) plot. SEs for GRM-SEM $h^2_{SNP}$ contributions have been omitted for clarity. **(C)** Genetic correlations with liability to Asperger. **(D)** Path diagram of an extended GRM-SEM IPC model mapping the polygenic score for educational attainment ($PGS_{EA}$) onto the model structure of the best-fitting ($S_{ALL}$, Figure 3H) SPARK model. **(E)** Corresponding standardised genetic variance (GRM-SEM $h^2_{SNP}$) plot. SEs for GRM-SEM $h^2_{SNP}$ contributions have been omitted for clarity. **(F)** Genetic correlations with the $PGS_{EA}$. **(A,D)** Observed measures are represented by squares and latent variables by circles ($A_{lang}$/$A_{dev}$/$A_{beh}$: shared genetic factor, AS: specific genetic factor, E: residual factor). Dotted and solid single-headed arrows (factor loadings) define

relationships between variables with $p>0.05$ and $p\leq0.05$, respectively. The genetic part of the model has been modelled using an Independent Pathway model, and the residual part using a Cholesky model (grey).

*Abbreviations:* $A_{lang}$ (Genetic language factor), $A_{dev}$ (Genetic developmental-delay factor), $A_{beh}$ (Genetic behavioural-problems factor), DCDQ (Developmental Coordination Disorder Questionnaire), $h^2_{SNP}$ (Single nucleotide polymorphism-based heritability), IPC (Independent Pathway-Cholesky GRM-SEM model), ODD (Oppositional Defiant Disorder), RBSR (Repetitive Behaviours Scale-Revised), $r_g$ (genetic correlation).

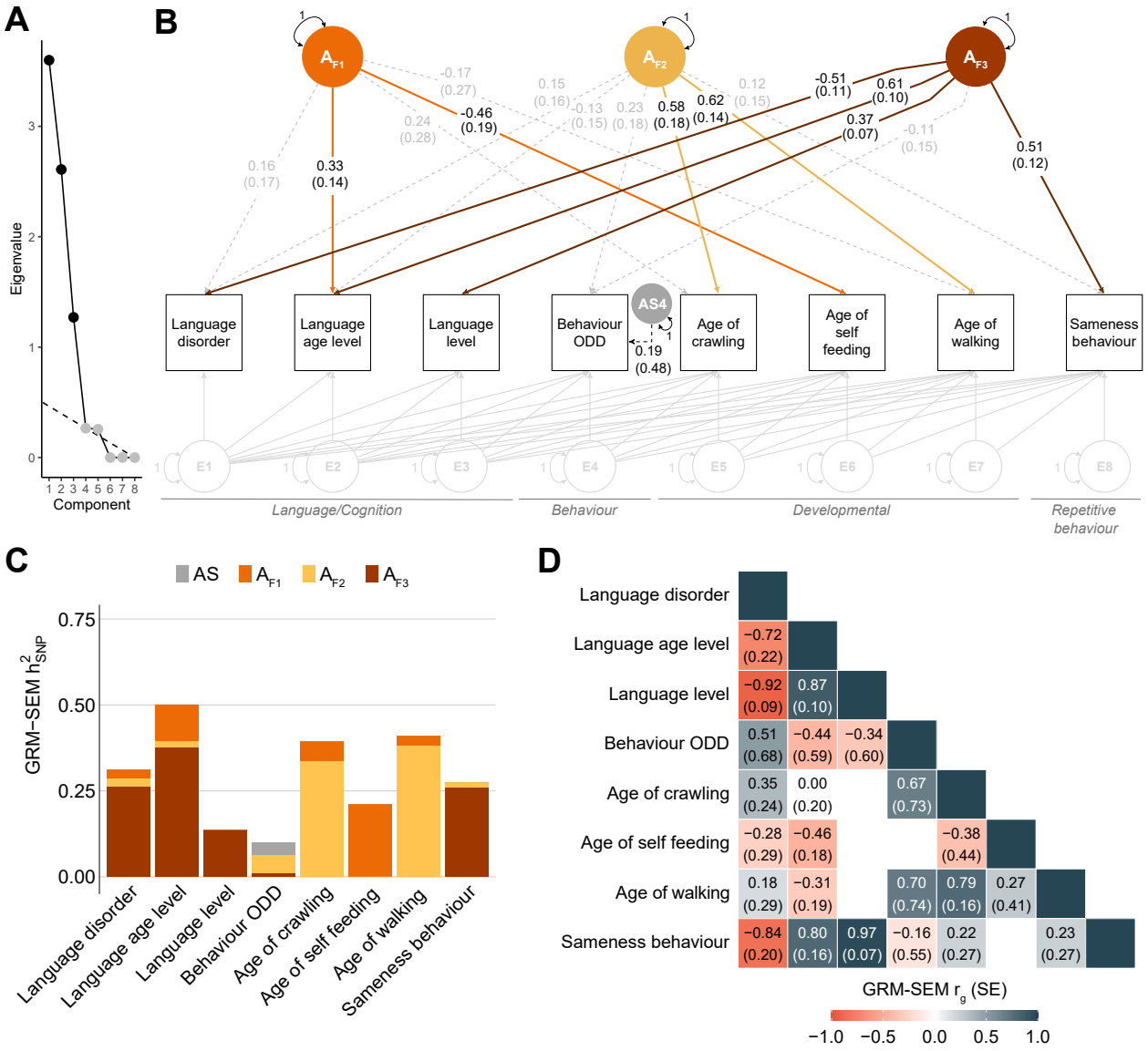


**Figure 6. Follow-up multi-factor GRM-SEM model in the SSC ($S_{ssc}$). (A)** Scree plot based on the eigenvalue decomposition of genetic correlations derived from a GRM-SEM Cholesky model, depicting the number of estimated shared genetic factors (in black) according to an optimal coordinate criterion. The dashed line indicates the "scree" of the plot (grey). **(B)** Path diagram depicting the best-fitting multi-dimensional GRM-SEM IPC model based on largely comparable phenotypes as studied in SPARK. Observed measures are represented by squares and latent variables by circles (A: shared genetic factor, AS: specific genetic factor, E: residual factor). Dotted and solid single-headed arrows (factor loadings) define relationships between variables with p>0.05 and p≤0.05, respectively. The genetic part of the model has been modelled using an Independent Pathway model, and the residual part using a Cholesky model (grey). **(C)** Corresponding standardised genetic variance (GRM-SEM $h^2_{SNP}$) plot. SEs for GRM-SEM $h^2_{SNP}$

746 contributions have been omitted for clarity. **(D)** Corresponding correlogram of genetic correlations.
747 Numeric values for genetic correlations that are not predicted by the genetic model structure were
748 omitted.

749 *Abbreviations*: $A_{F1,2,3}$ (Genetic factor 1,2,3), $h^2_{SNP}$ (Single nucleotide polymorphism-based
750 heritability), IPC (Independent Pathway-Cholesky GRM-SEM model), ODD (Oppositional Defiant
751 Disorder), $r_g$ (genetic correlation).

## DATA AVAILABILITY

Genotype and phenotype data from the SPARK and SSC cohorts are available upon application and approval from the Simons Foundation Autism Research Initiative (SFARI) (https://www.sfari.org/resource/autism-cohorts/). Approved researchers can obtain the SPARK and SSC population dataset described in this study by applying at https://base.sfari.org . GWAS summary statistics for educational attainment were accessed through the Social Science Genetic Association Consortium (SSGAC, https://thessgac.com/).

## CODE AVAILABILITY

In this study, we used the following software packages: PLINK (PLINK v1.9, https://www.cog-genomics.org/plink/1.9/), PRScs (https://github.com/getian107/PRScs), GCTA-GREML (GCTA v1.93, https://cnsgenomics.com/). We used the following R packages: stats 4.0.2, base 4.0.2, nFactors 2.4.1, psych 2.2.3, lavaan 0.6-10, grmsem 1.1.2 (https://gitlab.gwdg.de/beate.stpourcain/grmsem).

## ACKNOWLEDGMENTS

We are grateful to all of the families in SPARK, the SPARK clinical sites and SPARK staff. We are grateful to all of the families at the participating Simons Simplex Collection (SSC) sites, as well as the principal investigators (A. Beaudet, R. Bernier, J. Constantino, E. Cook, E. Fombonne, D. Geschwind, R. Goin-Kochel, E. Hanson, D. Grice, A. Klin, D. Ledbetter, C. Lord, C. Martin, D. Martin, R. Maxim, J. Miles, O. Ousley, K. Pelphrey, B. Peterson, J. Piggot, C. Saulnier, M. State, W. Stone, J. Sutcliffe, C. Walsh, Z. Warren, E. Wijsman). We appreciate obtaining access to phenotypic and genetic data on SFARI Base. This work was supported by a grant from the Simons Foundation Autism Research Initiative (SFARI ID: 514787, PI B.S.P.) covering the work of L.H., M.B. and M.M.J.D, in addition to support from the Max Planck Society. F.S., E.V., S.E.F. and B.S.P. were fully supported by the Max Planck Society. C.Y.S. was supported by the UK Medical Research Council (MRC) Integrative Epidemiology Unit at the University of Bristol (MC_UU_00011/3). J.B. was supported by the EU-AIMS and AIMS-2-TRIALS programmes which receive support from Innovative Medicines Initiative Joint Undertaking Grant No. 115300 and 777394, the resources of which are composed of financial contributions from the European Union's FP7 and Horizon2020 Programmes, and from the European Federation of Pharmaceutical Industries and Associations (EFPIA) companies' in-kind contributions, and

AUTISM SPEAKS, Autistica and SFARI; and by the Horizon2020 supported programme CANDY (Grant No. 847818).

## CONFLICT OF INTEREST

The authors declare no competing interests.

# REFERENCES


1. Havdahl A, Niarchou M, Starnawska A, Uddin M, van der Merwe C, Warrier V. Genetic contributions to autism spectrum disorder. Psychol Med. 51(13):2260–73.

2. Lord C, Brugha TS, Charman T, Cusack J, Dumas G, Frazier T, et al. Autism spectrum disorder. Nat Rev Dis Primers. 2020 Jan 16;6(1):1–23.

3. American Psychiatric Association. Diagnostic and Statistical Manual of Mental Disorders, DSM-IV. 4th ed. Washington, DC: American Psychiatric Press; 1994.

4. Lai M-C, Kassee C, Besney R, Bonato S, Hull L, Mandy W, et al. Prevalence of co-occurring mental health diagnoses in the autism population: a systematic review and meta-analysis. The Lancet Psychiatry. 2019 Oct 1;6(10):819–29.

5. Grove J, Ripke S, Als TD, Mattheisen M, Walters RK, Won H, et al. Identification of common genetic risk variants for autism spectrum disorder. Nature Genetics. 2019 Mar;51(3):431–44.

6. Weiner DJ, Wigdor EM, Ripke S, Walters RK, Kosmicki JA, Grove J, et al. Polygenic transmission disequilibrium confirms that common and rare variation act additively to create risk for autism spectrum disorders. Nature Genetics. 2017 Jul;49(7):978–85.

7. Gaugler T, Klei L, Sanders SJ, Bodea CA, Goldberg AP, Lee AB, et al. Most genetic risk for autism resides with common variation. Nature Genetics. 2014 Aug;46(8):881–5.

8. Warrier V, Zhang X, Reed P, Havdahl A, Moore TM, Cliquet F, et al. Genetic correlates of phenotypic heterogeneity in autism. Nat Genet. 2022 Jun 2;1–12.

9. Antaki D, Guevara J, Maihofer AX, Klein M, Gujral M, Grove J, et al. A phenotypic spectrum of autism is attributable to the combined effects of rare variants, polygenic risk and sex. Nat Genet. 2022 Jun 2;1–9.

10. Wigdor EM, Weiner DJ, Grove J, Fu JM, Thompson WK, Carey CE, et al. The female protective effect against autism spectrum disorder. Cell Genomics. 2022 Jun 8;2(6):100134.

11. Klei L, Sanders SJ, Murtha MT, Hus V, Lowe JK, Willsey AJ, et al. Common genetic variants, acting additively, are a major source of risk for autism. Mol Autism. 2012 Oct 15;3(1):9.

12. Thomas TR, Koomar T, Casten LG, Tener AJ, Bahl E, Michaelson JJ. Clinical autism subscales have common genetic liabilities that are heritable, pleiotropic, and generalizable to the general population. Transl Psychiatry. 2022 Jun 13;12(1):1–14.

13. Eyring KW, Geschwind DH. Three decades of ASD genetics: building a foundation for neurobiological understanding and treatment. Human Molecular Genetics. 2021 Oct 15;30(20):R236–44.

14. Leppa VM, Kravitz SN, Martin CL, Andrieux J, Le Caignec C, Martin-Coignard D, et al. Rare Inherited and De Novo CNVs Reveal Complex Contributions to ASD Risk in Multiplex Families. The American Journal of Human Genetics. 2016 Sep 1;99(3):540–54.

15. St Pourcain B, Eaves LJ, Ring SM, Fisher SE, Medland S, Evans DM, et al. Developmental Changes Within the Genetic Architecture of Social Communication Behavior: A Multivariate Study of Genetic Variance in Unrelated Individuals. Biological Psychiatry. 2018 Apr 1;83(7):598–606.

16. Shapland CY, Verhoef E, Davey Smith G, Fisher SE, Verhulst B, Dale PS, et al. Multivariate genome-wide covariance analyses of literacy, language and working memory skills reveal distinct etiologies. npj Science of Learning. 2021 Aug 19;6(1):1–12.

17. Feliciano P, Daniels AM, Green Snyder L, Beaumont A, Camba A, Esler A, et al. SPARK: A US Cohort of 50,000 Families to Accelerate Autism Research. Neuron. 2018 Feb 7;97(3):488–93.

18. Fischbach GD, Lord C. The Simons Simplex Collection: A Resource for Identification of Autism Genetic Risk Factors. Neuron. 2010 Oct 21;68(2):192–5.

19. Yang J, Lee SH, Goddard ME, Visscher PM. GCTA: a tool for genome-wide complex trait analysis. Am J Hum Genet. 2011 Jan 7;88(1):76–82.

20. Lee SH, Yang J, Goddard ME, Visscher PM, Wray NR. Estimation of pleiotropy between complex diseases using single-nucleotide polymorphism-derived genomic relationships and restricted maximum likelihood. Bioinformatics. 2012 Oct 1;28(19):2540–2.

21. Brown JD. Choosing the Right Type of Rotation in PCA and EFA. Shiken: JALT Testing & Evaluation SIG Newsletter. 2009 Nov;13(3):20–5.

22. Wray NR, Lee SH, Kendler KS. Impact of diagnostic misclassification on estimation of genetic correlations using genome-wide genotypes. Eur J Hum Genet. 2012 Jun;20(6):668–74.

23. Minshawi NF, Hurwitz S, Fodstad JC, Biebl S, Morriss DH, McDougle CJ. The association between self-injurious behaviors and autism spectrum disorders. Psychol Res Behav Manag. 2014 Apr 12;7:125–36.

24. Maddox BB, Trubanova A, White SW. Untended wounds: Non-suicidal self-injury in adults with autism spectrum disorder. Autism. 2017 May 1;21(4):412–22.

25. Moseley RL, Gregory NJ, Smith P, Allison C, Baron-Cohen S. A 'choice', an 'addiction', a way 'out of the lost': exploring self-injury in autistic people without intellectual disability. Molecular Autism. 2019 Apr 11;10(1):18.

26. Grotzinger AD, Rhemtulla M, de Vlaming R, Ritchie SJ, Mallard TT, Hill WD, et al. Genomic structural equation modelling provides insights into the multivariate genetic architecture of complex traits. Nat Hum Behav. 2019 May;3(5):513–25.

27. American Psychiatric Association. Diagnostic and statistical manual of mental disorders. 5th ed. Washington, DC: American Psychiatric Association; 2013.

28. Okbay A, Beauchamp JP, Fontana MA, Lee JJ, Pers TH, Rietveld CA, et al. Genome-wide association study identifies 74 loci associated with educational attainment. Nature. 2016 May;533(7604):539–42.

29. Marioni RE, Ritchie SJ, Joshi PK, Hagenaars SP, Okbay A, Fischer K, et al. Genetic variants linked to education predict longevity. PNAS [Internet]. 2016 Nov 22 [cited 2017 Nov 21];113(47):13366–71. Available from: http://www.pnas.org/content/113/47/13366

30. Tager -Flusberg Helen. Risk Factors Associated With Language in Autism Spectrum Disorder: Clues to Underlying Mechanisms. Journal of Speech, Language, and Hearing Research. 2016 Feb;59(1):143–54.

31. Carruth BR, Ziegler PJ, Gordon A, Hendricks K. Developmental milestones and self-feeding behaviors in infants and toddlers. Journal of the American Dietetic Association. 2004 Jan 1;104:51–6.

32. Zubler JM, Wiggins LD, Macias MM, Whitaker TM, Shaw JS, Squires JK, et al. Evidence-Informed Milestones for Developmental Surveillance Tools. Pediatrics. 2022 Feb 8;149(3):e2021052138.

33. Webber C, Blissett J, Addessi E, Galloway AT, Shapiro L, Farrow C. An infant-led approach to complementary feeding is positively associated with language development. Maternal & Child Nutrition. 2021;17(4):e13206.

34. CDC. What is a Developmental Milestone? [Internet]. Centers for Disease Control and Prevention. 2022 [cited 2022 Jun 16]. Available from: https://www.cdc.gov/ncbddd/actearly/milestones/index.html

35. Hannigan LJ, Askeland RB, Ask H, Tesli M, Corfield E, Ayorech Z, et al. Developmental milestones in early childhood and genetic liability to neurodevelopmental disorders. Psychological Medicine. 2021 Sep;1–9.

36. Munafò MR, Tilling K, Taylor AE, Evans DM, Davey Smith G. Collider scope: when selection bias can substantially influence observed associations. International Journal of Epidemiology. 2018 Feb 1;47(1):226–35.

37. Chang TS, Cirnigliaro M, Arteaga SA, Pérez-Cano L, Ruzzo EK, Gordon A, et al. The Contributions of Rare Inherited and Polygenic Risk to ASD in Multiplex Families. medRxiv. 2022 Apr 16;2022.04.05.22273459.

38. Chang CC, Chow CC, Tellier LC, Vattikuti S, Purcell SM, Lee JJ. Second-generation PLINK: rising to the challenge of larger and richer datasets. GigaScience. 2015 Dec 1;4(1):s13742-015-0047–8.

39. Rutter M, Bailey A, Lord C. The Social Communication Questionnaire: Manual. Los Angeles, CA : Western Psychological Services; 2003.

40. Lam KSL, Aman MG. The Repetitive Behavior Scale-Revised: Independent Validation in Individuals with Autism Spectrum Disorders. J Autism Dev Disord. 2007 May 1;37(5):855–66.

41. Wilson BN, Crawford SG, Green D, Roberts G, Aylott A, Kaplan BJ. Psychometric Properties of the Revised Developmental Coordination Disorder Questionnaire. Physical & Occupational Therapy In Pediatrics. 2009 Jan 1;29(2):182–202.

42. Achenbach TM, Rescorla LA. Manual for the ASEBA school-age forms & profiles: child behavior checklist for ages 6-18, teacher's report form, youth self-report: an integrated system of multi-informant assessment. University of Vermont, research center for children youth & families; 2001.

43. Lord C, Rutter M, DiLavore PC, Risi S. Autism diagnostic observation schedule: ADOS manual. Western Psychological Corporation; 2008.

44. Price AL, Patterson NJ, Plenge RM, Weinblatt ME, Shadick NA, Reich D. Principal components analysis corrects for stratification in genome-wide association studies. Nat Genet. 2006 Aug;38(8):904–9.

45. Sofer T, Zheng X, Gogarten SM, Laurie CA, Grinde K, Shaffer JR, et al. A fully adjusted two-stage procedure for rank-normalization in genetic association studies. Genetic Epidemiology. 2019;43(3):263–75.

46. Martin NG, Eaves LJ. The genetical analysis of covariance structure. Heredity. 1977 Feb;38(1):79–95.

47. Verhulst B, Prom-Wormley E, Keller M, Medland S, Neale MC. Type I Error Rates and Parameter Bias in Multivariate Behavioral Genetic Models. Behav Genet [Internet]. 2019 Jan [cited 2020 Dec 4];49(1):99–111. Available from: http://link.springer.com/10.1007/s10519-018-9942-y

48. Gorsuch RL. Factor analysis. 2nd ed. Hillsdale, NJ: Lawrence Erlbaum Associates; 1983.

49. Holzinger KJ, Swineford S. The Bi-factor method. Psychometrika. 1937;47:41–54.

50. Gibbons R. Bi-factor Analysis. In: Michalos AC, editor. Encyclopedia of Quality of Life and Well-Being Research. Dordrecht: Springer Netherlands; 2014. p. 386–94.

51. Hastie T, Tibshirani R, Friedman J. The Elements of Statistical Learning: Data Mining, Inference, And Prediction. 2nd ed. Springer Series in Statistics; 2009.

52. Falconer DS, Mackay F. Introduction to Quantitative Genetics. In: Introduction to Quantitative Genetics. 1996. p. 464–464.

53. Hotelling H. Analysis of a complex of statistical variables into principal components. Journal of Educational Psychology. 1933;24(6):417–41.

54. Raîche G, Walls TA, Magis D, Riopel M, Blais J-G. Non-graphical solutions for Cattell's scree test. Methodology: European Journal of Research Methods for the Behavioral and Social Sciences. 20130218;9(1):23.

55. Kaiser HF. The Application of Electronic Computers to Factor Analysis. Educational and Psychological Measurement. 1960 Apr 1;20(1):141–51.

56. Guttman L. Some necessary conditions for common-factor analysis. Psychometrika. 1954 Jun;19(2):149–61.

933 57. Cattell RB. The Scree Test For The Number Of Factors. Multivariate Behavioral Research.
934 1966 Apr 1;1(2):245–76.

935 58. Lawley DN, Maxwell AE. Factor analysis as a statistical method. 2nd ed. London:
936 Butterworths; 1971.

937 59. Rosseel Y. lavaan: An R Package for Structural Equation Modeling. J Stat Soft. 2012 May
938 24;48(2):1–36.

939 60. Mîndrilă D. Maximum Likelihood (ML) and Diagonally Weighted Least Squares (DWLS)
940 Estimation Procedures: A Comparison of Estimation Bias with Ordinal and Multivariate Non-
941 Normal Data. IJDS. 2010 Mar 1;1(1):60–6.

942 61. Kline RB. Principles and Practice of Structural Equation Modeling. New York, NY: The
943 Guilford Press; 2016.

944 62. Revelle W. psych: Procedures for Psychological, Psychometric, and Personality Research
945 [Internet]. Evanston, Illinois: Northwestern University; 2022. Available from: https://CRAN.R-
946 project.org/package=psych

947 63. Nyholt DR. A Simple Correction for Multiple Testing for Single-Nucleotide Polymorphisms in
948 Linkage Disequilibrium with Each Other. The American Journal of Human Genetics. 2004
949 Apr 1;74(4):765–9.

950 64. Choi SW, Mak TS-H, O'Reilly PF. Tutorial: a guide to performing polygenic risk score
951 analyses. Nat Protoc. 2020 Sep;15(9):2759–72.

952 65. Lee JJ, Wedow R, Okbay A, Kong E, Maghzian O, Zacher M, et al. Gene discovery and
953 polygenic prediction from a genome-wide association study of educational attainment in 1.1
954 million individuals. Nat Genet. 2018 Aug;50(8):1112–21.

955 66. Ge T, Chen C-Y, Ni Y, Feng Y-CA, Smoller JW. Polygenic prediction via Bayesian regression
956 and continuous shrinkage priors. Nat Commun. 2019 Apr 16;10(1):1776.

957